A EUROPEAN JOURNAL

CHEMPHYSCHEM

OF CHEMICAL PHYSICS AND PHYSICAL CHEMISTRY

Accepted Article

Title: Insight into Excitation Dependent Fluorescence of Carbon Dots

Authors: Divya Sasi, Satya Narayan, Sri Rama Koti Ainavarapu, and Deepa Khushalani

To be cited as: *ChemPhysChem* 10.1002/cphc.201801061

Link to VoR: http://dx.doi.org/10.1002/cphc.201801061

A Journal of

ChemPubSoc Europe

WILEY-VCH

www.chemphyschem.org

WILEY-VCH

ARTICLE

Insight into Excitation Dependent Fluorescence of Carbon Dots

S.Divya, Satya Narayan, Sri Rama Koti Ainavarapu* and Deepa Khushalani*

Abstract: High quantum yield, photoluminescence tunability, and sensitivity to the environment are the few distinct trademarks that make carbon nanodots (CDs) interesting for fundamental research with potential to replace the prevalent inorganic semiconductor quantum dots. Currently, application and fundamental understanding of CDs are constrained because it is difficult to make a quantitative comparison among different types of CDs simply because their PL properties are directly linked to their size distribution, the surface functionalization, the carbon core structures (graphitic or amorphous) and the number of defects. Herein, we report a facile one-step synthesis of mono-dispersed and highly fluorescent nanometre size CDs from a 'family' of glucose-based sugars. These CDs are stable in aqueous solutions with photoluminescence in the visible range. Our results show several common features in the family of CDs synthesized in that the fluorescence, in the visible region, is due to a weak absorption in the 300-400 nm from a heterogeneous population of fluorophores. Fluorescence quenching experiments suggest the existence of not only surface-exposed fluorophores but more importantly solvent inaccessible fluorophores present within the core of CDs. Interestingly, time-resolved fluorescence anisotropy experiments directly suggest that a fast exchange of excitation energy occurs that results in a homo-FRET based depolarization within 150ps of excitation.

Introduction

Since their inception, carbon dots (CDs) have emerged as an intriguing class of photoactive nanomaterials attracting considerable attention. Despite the absence of classically defined quantum confinement, their fluorescence properties are impressive as they are known to display excitation dependent emission irrespective of their sizes. As such, they are being promoted as the next generation of luminescent materials simply because of their properties such as high luminescence, chemical solubility, facile surface modification, biocompatibility, high resistance to photobleaching and low cost. Many of the aforementioned aspects are in fact superior to conventional fluorescent organic dyes and luminescent inorganic quantum dots, and hence CDs are being actively pursued in a wide variety of applications. [1-3]

Despite this immense interest, it is intriguing however to note that the exact cause and nature of their excitation-dependent fluorescence, which actually violates the Kasha-Vavilov's rule of excitation independent emission luminescence, is still not fully understood and in fact to date there still is a lack of consensus as to the origin of this emission. This aspect has been addressed by various groups by analyzing, for example, the role of surface groups on emission, size variation, co-excitation of the CDs in different emissive states, evaluating the charge transfer dynamics in presence of surrounding molecules/ions, or assessing the pH dependence of fluorescence of these CDs. However, despite this large effort, it is apparent that a cohesive and detailed conceptual understanding of the exact origin of fluorescence and more importantly its correlation with the CD chemical structure is still lacking.[4-11] Majority of the studies indicate that photoluminescence (PL) is mainly a surface phenomenon and the properties are due to a variety of defective functional groups present solely on the surface. The carbon core is being conceptualized as either an amorphous or a graphitic structure and in principle devoid of any PL properties.[10]

One of the major difficulties in collating data from different published reports has been the large heterogeneity in the synthesis of the CDs. The precursors used are highly diverse in their structures ranging from well-defined molecules such as ascorbic acid to complex configurations such as grass or even hair fiber.[12] These have then been exposed to a myriad of conditions, involving large pH ranges and or additives/solvents (that may or may not be inert in terms of affecting the PL of the ensuing structures). Moreover, despite considerable research efforts that have been expended to produce CDs with controlled dimensions and surface properties (using a variety of techniques including chemical and thermal oxidation, laser ablation, microwave processing, template methods and deoxygenation of natural carbon sources) there is still a lack of a unifying theory on PL.[13] It is, in fact, difficult to make a quantitative comparison among different types of CDs simply because their PL properties are directly linked to their size distribution, the surface functionalization, the carbon core structures (graphitic or amorphous) and the number of defects. These in turn are highly sensitive to the precursors and the synthesis conditions used. Hence it is has become apparent that in order to elucidate the PL aspects in a detailed manner, it is imperative that the composition and structure of the CDs have to be carefully controlled and this is crucial for understanding their complex luminescence mechanism.

To address these issues, presented here is a systematic study whereby a carefully controlled range of CDs have been synthesized in a facile manner without interference of additives. The synthesis is highly versatile employing a range of six individual precursors which belong to the same 'family' of sugars. The only alteration has been their molecular weight and number/type of functional groups. The structures are shown in figure 1 below and it can be seen that they range from a monomeric unit to a well-defined polymer consisting of specifically a seven-membered ring of glucose (β-cyclodextrin). Importantly,

Department of Chemical Sciences, Tata Institute of Fundamental Research, Homi Bhabha Road, Colaba, Mumbai 400 005, India. khushalani@tifr.res.in; koti@tifr.res.in

Supporting information for this article is given via a link at the end of the document.

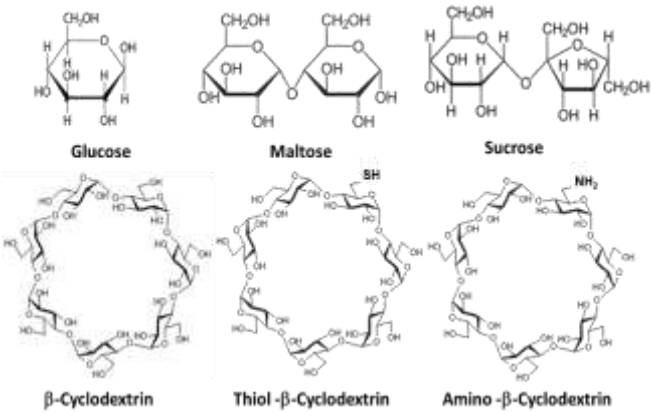

Figure 1: Structure of the different CD precursors.

specifically, only one –OH moiety of β-cyclodextrin has been altered to either a -SH or -NH_2 such that direct insight can be gained into effect of the functionality (-OH vs -SH vs -NH_2) on the optical properties. A trivial synthetic protocol has been employed to form CDs that uses only water as the solvent under microwave pyrolysis without the addition of any other acid, base, reducing/oxidizing agent or even capping agent. Subsequently, spectroscopic studies have been performed to evaluate the photo-physics of the synthesized CDs and inferences have been obtained in regard to how the structure of the precursor dictates the final composition of the CDs and hence their optical properties. Based on the experimental results we assume that the PL origin mainly arise not only from the chemical groups on the surface electronically coupled to the carbon core but also due to coupling between the intrinsic defects in the core and the surface states forming molecular fluorophores.

Results and Discussion

The as-synthesized colloidal suspensions of CDs obtained were characterized within at least 24 hrs. Irrespective of this aspect, however it should be noted that the CDs were stable for up-to two months as the data obtained within this period was always reproducible. Photoluminescence spectra were recorded before and after dialysis with no visible differences. Hence our protocol proves to be facile and purification free method for synthesizing carbon dots. Figure 2a displays a TEM image of Glucose CDs. It is observed that the particles are spherical in nature with a narrow size distribution centered at *ca*. 4 nm and table 1 shows the average size determined for all the precursors used (data collated from figure S3). It can be surmised that shape, size and size distribution are correspondingly similar irrespective of the precursors used for CD synthesis. As the CDs had monodispersed nanometer size distribution, in order to get insight into the chemical structure and molecular weight of the CDs, MALDI analysis was performed, figure 2b (additional data in figure S4). For these MALDI measurements, the incident laser wavelength used was 337 nm, therefore it is expected that the CDs have minimal direct absorption and in fact the matrix (α-Cyano-4-hydroxycinnamic acid) are in fact assisting the desorption of CDs during acquisition. As such the MALDI data represents in principle not a fragmentation pattern but instead it is a representation of particle weight heterogeneity. The pattern in the mass spectrum of Glucose CDs displayed a m/z range of 800-1200 which was analogous to the ranges for the other CDs that were synthesized. Similar to TEM, results from MALDI also exhibited an intriguing trend among all the products in that similarly spaced mass differences were observed irrespective of the precursor used, indicating that the entire set of CDs synthesized had a large similarity in their final molecular structure. Dramatic differences were not observed and in fact the highest m/z obtained from all the different CDs are compiled in table 1 and these were found to be comparable and centered at a value of *ca*. 1150. Moreover, the pattern in all the six CDs synthesized showed common mass differences of peaks whose values were at 14, 17, 28, 32, 44 m/z corresponding to the mass difference of a methyl (-CH_3) or a hydroxyl (-OH) group, aldehyde (-CHO), methoxy (-OCH_3) and carboxylic group (-COOH) respectively. The only major difference observed was that in the data of CDs synthesized from β-Cyclodextrin-SH, a peak observed at m/z value of 47 which could be ascribed to methanethiolate (-CH_3S) whereas in β-Cyclodextrin-NH_2, the MALDI pattern had the most number of new peaks and specifically one that was observed at Δm/z value of 17 which could be ascribed due to the loss of amino (-NH_2) group.

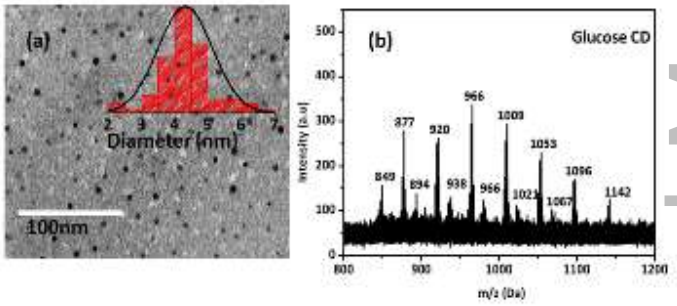

Figure 2: (a) TEM image and particle size distribution histogram of the carbon dots from Glucose. (b) MALDI-TOF MS of CDs synthesised from Glucose.

For further structural insight, X-ray diffraction studies were performed on the lyophilized samples figure S5. The diffractogram displays a single peak at *ca*. 3.8 Å (similar to the reports published by other groups)[14,15] and as it is larger than the interlayer spacing for the conventional (002) planes of bulk graphite (3.34 Å), it can therefore be deduced that the CD framework consists of a turbostratic carbon structure having a disordered graphitic plane alignment. In the FTIR spectra, figure S6, there were practically negligible differences observed between the six CDs synthesized and all the spectra consistently displayed peaks at *ca*. 3300, 2900 and 1600 cm^{-1} which could be assigned to the O-H, C-H, C=C symmetric stretch of the carbon skeleton.

In order to evaluate the optical properties of the CDs, UV-Vis absorption spectra were acquired, figure 3. Again, it can be observed that the CDs prepared from different carbon sources

Sample	Average size (nm)	Mol. Mass of Precursor (g/mol)	Highest m/z (g/mol)	PL Emission Range (nm)
Glucose CD	4.3 ± 0.8	180	1142	430-555
Sucrose CD	4.2 ± 1.2	342	1184	433-553
Maltose CD	4.2 ± 1.1	360	1168	439-553
β-Cyclodextrin CD	4.0 ± 0.9	1135	1191	432-556
β-Cyclodextrin-SH CD	4.4 ± 0.9	1151	1168	432-549
β-Cyclodextrin-NH_2 CD	3.8 ± 0.9	1134	1196	435-541

Table 1: Size and fluorescence properties of CDs

gave similar absorption features. It needs to be clearly stated that the as-synthesized product, after microwave synthesis, was diluted 5 times (consistently for each of the six CDs) and then the absorption spectrum was acquired. A strong band at 220 nm was observed and it is known to originate from the π→π* transition of the aromatic carbons that are normally hypothesized to be present in the core.[16] The broad intense peak at 280 nm can be assigned to the typical absorption of an n→π* transition which is again due to the structural motif and has been observed in CDs prepared from a variety of other precursors as well.[17] Other than these two strong features, the rest of the spectrum can be considered to consist of a long absorptive tail extending up to 800nm (see inset). The only difference between the data of the six CDs was not in the position of the absorption features but in fact the intensity of these bands. The β-Cyclodextrin-NH_2 based CDs gave the highest intensity of the bands while glucose-based CDs gave the least intense spectrum.

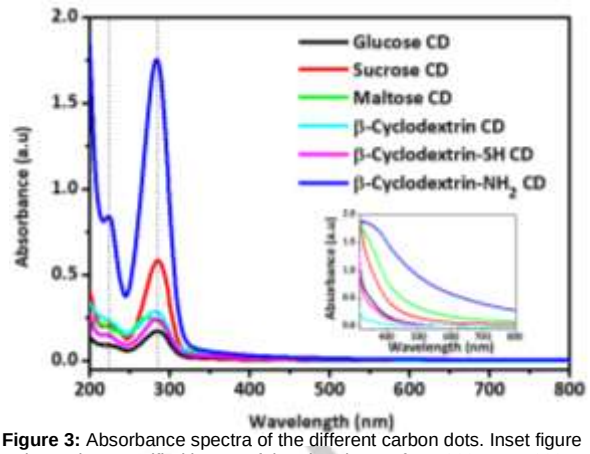

Figure 3: Absorbance spectra of the different carbon dots. Inset figure shows the magnified image of the absorbance from 360 nm to 800.

Further insight was obtained using photoluminescence measurements. Figure 4a shows the normalized steady state PL data for glucose CDs while being irradiated with a variety of excitation wavelengths ranging from 300 to 500 nm. Tuneable emission was observed with the most intense emission being

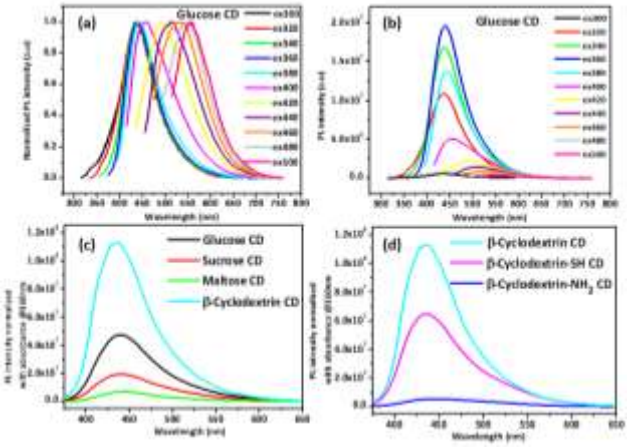

Figure 4: (a & b) Excitation dependent photoluminescence spectra of Glucose CDs. (c & d) Emission spectra of CDs excited at 360nm.

observed at 440 nm when the sample was excited with 360 nm, (figure 4 b, c & d). This behavior was observed for all the other 5 CDs (additional data in figure S7). Table 1 gives the tunable PL range of CDs from different precursors and the fluorescence peak position was found to vary in the range from 430-555 nm when the excitation wavelength was varied from 300-500 nm. Generally, such variable emission has been attributed to "defect states" with a broad energy distribution on either graphitized core of CDs or the oxygenated groups that are commonly present (such as carbonyl, carboxyl acid, ether *etc*.).[18] It was observed for our samples, that as the number of monomer units were increased in the precursor, initially the emission intensity of the corresponding CDs decreased *i.e*., from glucose to sucrose to maltose but the emission was augmented dramatically when the monomer unit increased to seven. Polymeric nature of β-cyclodextrin therefore had a beneficial effect on the PL intensity. Correspondingly, when the functional groups were varied, it was observed that replacing a hydroxyl group with either a thiol (-SH) or amino(-NH_2) group, the emission was significantly suppressed.

It needs to be highlighted that all the CDs exhibited an absence of fluorescence emission when excited at the maximum of the UV absorption band at 280nm. Such behavior is quite contrary to that of semiconductor quantum dots but has been commonly observed for CDs and also for graphene and graphene oxide nanoparticles. [19-21] It can therefore be postulated that there is a prevalence of two types of chromophores, non-emitting and those emitting in the visible range. The absorption coefficient of the carbon core is higher than that of the fluorophore species so that the relative absorption of the core is visible while that of the fluorophore appears to be suppressed. Figure S8 represents the excitation spectra of the CDs at emission wavelength of 440 nm. It is clearly visible that the excitation spectra have negligible resemblance to the UV-Vis absorption spectra. Hence, it can be surmised that the majority of the structure of the CDs consist of a turbostratic graphitic/amorphous carbon structure within which are embedded fluorophores. This large skeletal framework is not-fluorescent while there exists within it a heterogeneous population of fluorophores with excitation dependent emission spectra depending on their chemical structures.

To gain further insight into location and accessibility of these fluorophores, fluorescence quenching experiments were performed using two well-known quenchers: acrylamide and potassium iodide (KI). The Stern–Volmer plots in figure 5 demonstrate that both quenchers reduce the PL intensity in a concentration dependent manner and as the plots are predominantly linear it suggests that the quenching mechanism is either static or dynamic, but not both. Acrylamide is normally expected to quench both the ‘‘exposed’’ and ‘‘buried’’ fluorophores (as has been shown e.g. for buried tryptophan residues in proteins[22]), while iodide being charged, very large in size, and highly hydrated, is limited normally to quenching surface fluorophores. But here, KI seems to quench the PL to a larger extent (2-5 times) than acrylamide (1.5 - 2.5 times) for all the CDs except for β-cyclodextrin CD for which acrylamide appears to be a better quencher. The quenching constants determined are detailed in table 2 (individual PL spectra with quenchers KI and acrylamide are shown in figures S9 and S10).

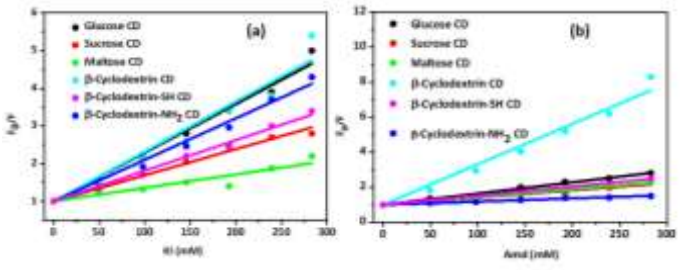

Figure 5: Steady state quenching of CDs with KI and acrylamide as quenchers.

A uniform decrease was observed in the PL intensity for the entire emission range for KI without any shift in the emission maxima. In contrast, the emission maxima were found to shift to longer wavelengths at elevated concentrations of acrylamide. The observed spectral red shift of *ca*. 5-20 nm in case of acrylamide quenching presumably results from the selective quenching of fluorophores more exposed to the solvent. Upon the suppression of these surface fluorophores, the buried species (which are not being as effectively quenched by acrylamide) are populating the emission spectrum and are now being more clearly observed. Thus, according to the above results CDs may be considered to have at least two populations of fluorophore species characterized by different fluorescence maxima and a differing accessibility to acrylamide.

To test, whether the fluorescence quenching is static or dynamic, we performed time-resolved fluorescence experiments. Normalized time resolved fluorescence curves and corresponding Stern-Volmer plots of CD-water dispersions are shown in figure 6a (additional data in figure S11, excitation wavelength used was 366 nm and emission was at 440 nm). All the fluorescence decay curves were fitted to multi-exponentials and mean fluorescence lifetimes (τ_m) were measured (for details see experimental section in Supporting Information). Mean lifetime and bimolecular quenching constants obtained are given in the table 2. It can be confirmed from this data that quenching is dynamic in nature. For all the six types of CDs, after the addition of KI, the lifetime of PL was observed to decrease as observed in table S1-S6. The fluorescence decays of CDs required multi-exponential fits suggesting heterogeneity of fluorescent species. It was observed that as we sequentially evaluate glucose CDs to β-cyclodextrin based CDs, the lifetime of the fastest component increased from 0.24 ns (50%) to 0.33 ns (39%) whereas the slowest component decreased from10.4 ns (1%) to 4.6 ns (6%). Upon variation of the functional groups, it could be observed that the fastest component had the shortest lifetime of 0.05 ns (62%) for β-cyclodextrin-NH_2 whereas the lifetime of the slowest component remained more or less the same with an overall decrease in the average lifetime. Furthermore, the estimated bimolecular quenching constant (K_q=K_{SV}/τ) from the Stern-Volmer constant (K_{SV}) and the mean lifetime in the absence of quencher (τ), were found to be large (0.5-2.5 x 10^{10}) suggesting that the quenching by KI was diffusion-controlled and very efficient.[23] Moreover, the linearity in the Stern-Volmer quenching plots without any saturation (or downward curvature) suggested that all the fluorophores, both the surface and in the core, were efficiently quenched.

The aforementioned observations raise an important question that how a solvated-iodide (from KI), which is larger than acrylamide, is able to quench buried fluorophores? How the buried fluorophores are quenched without physically colliding with iodide ions? This would only be possible if the excitation energy from the buried fluorophores is transferred to those at the surface which are then being quenched efficiently by the iodide. We further investigated this aspect using time-resolved fluorescence anisotropy experiments as detailed below.

Anisotropy studies based on time resolved fluorescence polarization is a powerful tool which provides valuable information on the size and shape of fluorescing particles, and characteristics of surrounding environment. This technique relies on the fact that linearly polarized light preferentially excites those molecules or particles whose transition dipole moment is parallel to the incident light field. Because of the rotational diffusion of the excited particles, their average emission dipole moment acquires a non-vanishing component perpendicular to the exciting field and the

Sample	Steady-state K_{SV} (M^{-1})		Time-resolved studies K_{SV} (M^{-1})	τ_0 (ns)	K_q ($M^{-1}s^{-1}$)
	KI	Acrylamide			
Glucose CD	13	7	24	1.1	21.8×10^9
Sucrose CD	7	4	7	0.65	10.8×10^9
Maltose CD	4	5	12	1.02	11.8×10^9
β-Cyclodextrin CD	13	22	7	1.33	5.3×10^9
β-Cyclodextrin-SH CD	8	6	18	0.83	21.7×10^9
β-Cyclodextrin-NH_2 CD	11	2	13	0.52	25×10^9

Table 2: Steady state and time-resolved fluorescence quenching properties of CDs.

same occurs to the polarization direction of fluorescence light. Fluorescence anisotropy decay curves of CDs system are shown in the figure 6b (additional data in figure S12). Initial anisotropy was observed to decrease with time due to the loss of initial

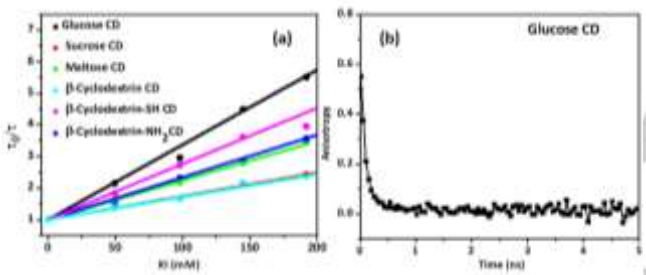

Figure 6: (a) Time-resolved fluorescence studies on quenching of CDs with KI. (b) Time-resolved fluorescence anisotropy Glucose-CD system.

orientation as a result of rotational diffusion or of energy transfer to other emitters. The distinction between these two depolarizing factors is crucial in the analysis of anisotropy decays of CDs. Our results demonstrate that in all studied systems there are fast anisotropy decays approximately equal to zero level with rotation correlational time constant ≤ *ca*. 150 ps in all the cases. In comparison, the rotations of globular protein molecules of similar size (4.5 nm) are observed in the range 5-10 ns.[24] In our case, instead of observing high anisotropy as expected from the rotation of CDs supposed to be in the 5-10ns range, the polarization decayed faster within 150ps. The observed very fast depolarization which is devoid of any molecular reorientation component suggests that the excitation energy of a fluorophore is being non-radiatively transferred to neighboring fluorophores that are oriented differently. So, it can be hypothesized that there exist donors and acceptors on the CD surface which are in different orientations and in the case of multiple transfers the information of initial polarization is lost through a homo-FRET mechanism. [21] It is possible that the fluorophores which are at the core of the CD transfer their excitation energy to their neighbours very quickly and this "appears" on the surface fluorophores during the energy transfer. As shown by the anisotropy studies, this is very fast and it also explains how KI is able to quench all the fluorophores uniformly even though some could be at the core and not physically accessible to the KI quencher. Moreover, the red-shift in the fluorescence maximum of CDs upon acrylamide quenching can now also be elucidated. As acrylamide is relatively less efficient compared to KI (table 2) by a factor of 2, when the excitation energy is transferred to the surface fluorophores it is red-shifted and is shown as emission because acrylamide is less efficient in quenching this, unlike KI which more effectively reduces all the emission. As such there is more uniform quenching throughout the emission spectra.

Conclusions

In summary, from the above data the following aspects can be surmised:

- PL increases when the precursor is changed from glucose to β-cyclodextrin. This suggests that polymeric materials are better precursors to form luminescent structures.
- In terms of functionality, the –OH moiety leads to more fluorescent CDs then either $–NH_2$ or –SH.
- For the final CDs that form, there are many "types" of fluorophores, some are buried and some are surface bound. Both types emit, albeit at different wavelengths and with different intensity.
- As such, it can be stated the CDs structures actually consist of a framework that has C=C and C=O moieties that are strongly absorbing but not emitting. Buried within this framework (in the bulk region as well as the surface) are a variety of chromophore species that absorb from 300 to 600 nm and each emits *ca*. between 430 to 560 nm.
- Our anisotropy results indicate that the fluorophores are interacting with each other through energy transfer and hence it can be deduced that depending on the raw precursor used there are a variety of fluorophores present on and beneath the surface.

Experimental Section

Materials: All precursors were procured with AR grade: D-glucose (SDFCL), Sucrose (SDFCL), Maltose Monohydrate (Loba Chemie), β-Cyclodextrin (ACROS Organics). All reagents of analytical reagent grade or above were used as received without any further purification.

Synthesis of mono-6-thio-β-Cyclodextrin

Mono-6-thio-β-Cyclodextrin was synthesised as adopted from the literature. [25] Briefly, 70 g β-Cyclodextrin was suspended in 500 ml water and 20 ml aqueous solution of 6.6 g NaOH solution was added dropwise which finally became transparent. 30 ml of 10.1 g p-toluene sulfonylchloride solution was added to the previous solution to form a white precipitate. The precipitate was removed by suction filtration and the filtrate was stored at 4°C. Resulting precipitate was separated and recrystallised. 2 g of the precipitate and 2 g thiourea was heated at reflux for two days in 100 ml methanol-water solution. The white solid obtained was added to methanol and stirred. The solid obtained after filtration was dissolved in 10 wt.% NaOH solution. The pH of the solution was adjusted to 2 with HCl, then 5 ml of trichloroethylene was added and stirred overnight and finally the precipitate was recovered by suction filtration and was washed with water. Structure and composition were confirmed with NMR and LCMS as shown in figures S1 and S2.

Synthesis of mono-6-amino-deoxy-6-β-Cyclodextrin

Mono-6-amino-deoxy-6-β-Cyclodextrin was synthesised from a procedure adapted from Tang et al. [26] 22 mmol of β-Cyclodextrin was added to 400 ml pyridine. 4 g p-toluenesulphonyl chloride was added to the mixture and stirred for 24 h. Solvent was removed, and the precipitate was stirred with acetone. Subsequent solid (solid I) was washed with acetone and recrystallized. 3.9 mmol of Solid I was added to 5 g sodium azide (76.9 mmol) along with 500 ml of deionized water and refluxed at 100°C. Precipitate was separated and 5 ml of 1,1,1,1-tetrachloroethane was added dropwise and stirred for 0.5 h. Solvent was evaporated to obtain a solid (solid II) which was recrystallized using hot water. 5 mmol of Solid II was refluxed with 5.5 mmol triphenylphosphine and 10 ml dimethyl formamide for 2 h at room temperature. 1 ml deionized water was then added and heated at 90°C for 3 h. Mixture was then cooled to room temperature and the final product was precipitated using acetone, washed and stored. Structure and composition were confirmed with NMR and LCMS as shown in figures S1 and S2.

Microwave pyrolysis method to prepare carbon dots

Synthesis was done by one step hydrothermal method in microwave oven at a pressure of 200 psi and a temperature of 175 °C with precursor concentration of 3.5 mmol in distilled water. The heating was done for 4hrs. During the synthesis no precipitate was observed. We ultra-centrifuged the samples at 35000 rpm but there was no distinct sedimentation. To confirm the purity, the samples were dialysed against pure water using dialysis membrane (1000 Da) for 24 hours. Each of the six precursors were processed separately yielding six different products. For XRD measurements, the synthesized colloidal solutions were lyophilized to obtain the corresponding CD solid phase.

Characterization

TEM analysis was done on a LIBRA 120, EFTEM Carl Zeiss. Matrix-assisted laser desorption/ionization (MALDI) measurements were performed on a TOF Bruker Daltonics Spectrometer. Low-resolution mass spectral analyses were carried out using a Shimadzu LCMS-2020 with an ESI probe (positive and negative ion modes). 1H NMR was collected in DMSO at 25°C on Varian 600 MHz. The UV-Vis absorption spectra were recorded using double beam PerkinElmer Lambda 750-UV/Vis/NIR spectrophotometer. FT-IR were recorded on a Nicolet-200-135 while Powder XRD measurements were recorded using a PAN analytical X'pertpro diffractometer with monochromatic Cu Kα source (λ = 1.54056 Å). All the steady state photoluminescent (PL) measurements were recorded using a SPEX Horiba Fluorolog fluorimeter.

Time-resolved Fluorescence: Fluorescence lifetime measurements and anisotropy decay kinetics were recorded by employing CW-passively mode-locked Nd:YLF laser (Millenia X, Spectra Physics, USA) driven Ti-sapphire pico-second laser (Spectra Physics, Mountain View, CA). Ti-sapphire pulses at 732 nm frequency doubled to 366 nm using GWU frequency doubler by Spectra Physics, USA, were used for exciting CDs. Fluorescence decay curves were obtained at a repetition rate of 8 MHz using a micro-channel plate photomultiplier (R2809u, Hamamatsu Corp.) coupled to the time-correlated single photon counting (TCSPC) setup. The full width at half maximum (FWHM) of the instrument response function (IRF) was ~40 ps. Fluorescence emission was measured at 440 nm using a combination of a monochromator and a 400 nm cut-off filter. Fluorescence intensity decay curves were collected from the sample after the excitation with the emission polarizer oriented at the magic angle (54.7º) with respect to the excitation polarizer. To optimize the signal-to-noise ratio, 10,000 photon counts were collected in the peak channel. For time-resolved anisotropy measurements, the emission data were collected at 0° (parallel fluorescence intensity, I ∥), and 90° (perpendicular fluorescence intensity, I ⊥) with respect to the excitation polarization. [27,28]

Acknowledgements

Authors are thankful to TIFR's TEM facility (Mr. Lalit Borde) and XRD facility (Nilesh Kulkarni). Mrs. Geetanjali Dhotre is also thanked for assistance with MALDI. The work at TIFR was supported through N-PDF Fellowship, SERB, Govt. of India (PDF/2016/000051) and DAE Plan funding.

Keywords: Carbon dots, Excitation dependent fluorescence, Lifetime, Anisotropy, Homo-FRET.

[1] Liu H, Ye T and Mao C, Angew. Chem. Int. Ed., **2007**, 46, 6473−6475.
[2] A, Baker SN and Baker GA Angew. Chem. Int. Ed., **2010**, 49, 6726−6744
[3] Zuo P, Lu X, Sun Z, Guo Y and He H, Microchimica Acta, **2016**, 183(2), 519-542.
[4] Li X, Wang H, Shimizu Y, Pyatenko A, Kawaguchi K and Koshizaki N, Chem. Comm., **2010**, 47(3), 932-934.
[5] Dhenadhayalan N, Lin KC, Suresh R and Ramamurthy P, J. Phys. Chem. C, 2016, 120(2), 1252-1261.
[6] Khan S, Gupta A, Verma NC and Nandi CK, Nano Lett., **2015**, 15(12), 8300-8305.
[7] Li H, He X, Kang Z, Huang H, Liu Y, Liu J, Lian S, Tsang CH, Yang X and Lee ST, Angew. Chem. Int. Ed., **2010**, 49(26), 4430-4434.
[8] Cao L, Anilkumar P, Wang X, Liu JH, Sahu S, Meziani MJ, Myers E and Sun YP, Can. J. Chem., **2010**, 89(2), 104-109.
[9] Wang X, Cao L, Lu F, Meziani MJ, Li H, Qi G, Zhou B, Harruff BA, Kermarrec F and Sun YP, Chem. Comm., **2009**, 25, 3774-3776.
[10] Shamsipur, Mojtaba, Ali Barati, and Sara Karami. Carbon,**2017**, 124, 429-472.
[11] Kong W, Wu H, Ye Z, Li R, Xu T and Zhang B, J. Lumin., **2014**, 148, 238-242.

[12] Lim, Shi Ying, Wei Shen, and Zhiqiang Gao. Chem. Soc. Rev., **2015**,44(1),362-381.
[13] Hu Q, Paau M. C, Zhang Y, Chan W, Gong X, Zhang L and Choi M. M., J. Chromatogr. A, **2013**, 1304, 234-240.
[14] Zhang, J., Shen, W., Pan, D., Zhang, Z., Fang, Y., and Wu, M., New J. Chem, **2010**, 34(4), 591-593.
[15] Puvvada, N., Kumar, B. P., Konar, S., Kalita, H., Mandal, M., and Pathak, A, Sci. Technol. Adv. Mater, **2012**, 13(4), 045008.
[16] Paredes, J. I., Villar-Rodil, S., Martinez-Alonso, A., and Tascon, J. M. D, Langmuir, **2008**, 24(19), 10560-10564.
[17] Hu, Q., Paau, M. C., Zhang, Y., Chan, W., Gong, X., Zhang, L., and Choi, M. M., J. Chromatogr. A, **2013**, 1304, 234-240.
[18] Deng, Y., Chen, X., Wang, F., Zhang, X., Zhao, D., and Shen, D, Nanoscale, **2014**, 6(17), 10388-10393.
[19] Jaiswal, A., Ghosh, S. S., and Chattopadhyay, A, Chem. Comm., **2012**, 48(3), 407-409.
[20] Lin, L. P., Wang, X. X., Lin, S. Q., Zhang, L. H., Lin, C. Q., Li, Z. M., and Liu, J. M, Spectrochim. Acta A, **2012**, 95, 555-561.
[21] Dekaliuk, M. O., Viagin, O., Malyukin, Y. V., and Demchenko, A. P, Phys. Chem. Chem. Phys., **2014**, 16(30), 16075-16084.
[22] Strambini, G. B., and Gonnelli, M., J. Chem. Phys. B, **2010**, 114(2), 1089-1093.
[23] J. R. Lakowicz, Principles of Fluorescence Spectroscopy, Springer, New York, 3rd edn, **2006**.
[24] Guo, X. Q., Castellano, F. N., Li, L., & Lakowicz, J. R., Anal. Chem., **1998**, 70(3), 632-637.
[25] Wang J, Kong L, Guo Z, Xu J and Liu J, J. Mater. Chem., **2010**, 20(25), 5271-5279.
[26] Tang W, & Ng S. C, Nat. Protoc., 2008, 3(4), 691-697.
[27] Mukhopadhyay S, Nayak, P. K., Udgaonkar, J. B. and Krishnamoorthy G., J. Mol. Biol., **2006**,358(4), 935-942.
[28] Jha A, Narayan S, Udgaonkar J. B, and Krishnamoorthy G, Biophys. J., **2012**, 103(4), 797-806.

10.1002/cphc.201801061

WILEY-VCH

Entry for the Table of Contents

ARTICLE

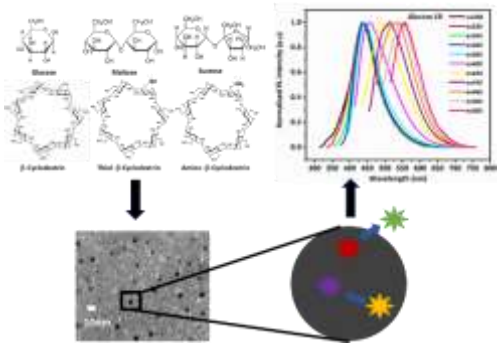

- Random dispersion of fluorophores
- Fast-FRET (<150 ps)
- Collisional quenching

*S. Divya, Satya Narayan, Sri Rama Koti Ainavarapu and Deepa Khushalani**

Page No. – Page No.

Insight into Excitation Dependent Fluorescence of Carbon Dots